

Research Article

End-Effector Trajectory Tracking Control of Space Robot with \mathcal{L}_2 Gain Performance

Haibo Zhang,^{1,2} Dayi Wang,^{1,2} Chunling Wei,^{1,2} and Bing Xiao³

¹Beijing Institute of Control Engineering, Beijing 100190, China

²National Key Laboratory of Science and Technology on Space Intelligent Control, Beijing 100190, China

³College of Engineering, Bohai University, Jinzhou 121013, China

Correspondence should be addressed to Haibo Zhang; zhanghb502@163.com

Received 17 April 2015; Accepted 6 September 2015

Academic Editor: Xinggang Yan

Copyright © 2015 Haibo Zhang et al. This is an open access article distributed under the Creative Commons Attribution License, which permits unrestricted use, distribution, and reproduction in any medium, provided the original work is properly cited.

This paper presents a novel solution to the control problem of end-effector robust trajectory tracking for space robot. External disturbance and system uncertainties are addressed. For the considered robot operating in free-floating mode, a Chebyshev neural network is introduced to estimate system uncertainties and external disturbances. An adaptive controller is then proposed. The closed-loop system is guaranteed to be ultimately uniformly bounded. The key feature of this proposed approach is that, by choosing appropriate control gains, it can achieve any given small level of \mathcal{L}_2 gain disturbance attenuation from external disturbance to system output. The tracking performance is evaluated through a numerical example.

1. Introduction

With the development and launch of spacecraft, the function of spacecrafts is becoming more and more complex. As a result, any component failure will deteriorate spacecraft's performance and sometimes even make the planned mission totally terminate. Aiming to decrease economic loss induced by spacecraft failures, on-orbit servicing has received considerable attentions. However, due to the harsh operating environment such as high temperature, it is very difficult for astronauts to accomplish orbital works. This makes space robot become the best option to accomplish orbital repair. Additionally, the space robot can also perform other on-orbit servicing missions such as repair, assembly, refueling, and/or upgrade of spacecraft. This leads to development of space robot techniques [1–6].

For space robot, the end-effector control in the presence of uncertain kinematics and dynamics is becoming one of the challenges that need to be addressed. In [7], the problem of uncertain kinematics in space robot's end-effector was investigated. In [8], a feedback control approach was presented to accomplish position and attitude control maneuver. The uncertainties in end-effector were addressed, and experimental results were given to verify the effectiveness

of the proposed controller. Taking control input saturation of end-effector's actuator into consideration, an adaptive controller was developed to perform trajectories tracking [9]. The tracking error was governed to be semiglobally asymptotic stable. On the other hand, on the standpoint of tracking control in mission space, many researchers have developed many effective control algorithms. In [10], an adaptive controller was presented to achieve tracking control of end-effector, and uncertain kinematics and dynamics were solved. The controller was able to guarantee the asymptotic stability of the closed-loop system, and ground test was also conducted to demonstrate its effectiveness. In [11], an adaptive control scheme without velocity measurements was developed. The demand of decreasing numbers of measurement sensors was satisfied, and the closed-loop tracking system was governed to be stable. In [12, 13], another novel adaptive controller was also synthesized in the presence of the dynamics of actuators, uncertain kinematics, and dynamics.

The preceding approaches were proposed based on the assumption that the dynamic model can be linearized. However, this assumption would not be satisfied for space robot. As a result, the above control methodologies were not applicable to space robot. Moreover, in the above nonlinear controller design, the developed controllers can only ensure

the stability of the resulted system. They were not able to achieve disturbance attenuation. It greatly limits the application of those schemes. To achieve tracking control with disturbance attenuation, \mathcal{L}_2 gain control approach is one of the most applied techniques [14–18].

Inspired by the great performance of \mathcal{L}_2 gain control, this work will investigate the problem of trajectory tracking control of space robot end-effector. Uncertain kinematics and dynamics will be addressed. To solve those uncertainties, Chebyshev neural network will be used to approximate those uncertainties, and an adaptive controller will be developed to compensate for these uncertainties. The main contribution of this work is that the desired trajectories can be followed with high accuracy, and \mathcal{L}_2 gain performance is achieved in the presence of external disturbances.

This paper is organized as follows. In Section 2 we recall some necessary notation, definitions, preliminary results, and the mathematical model used to investigate space robot end-effector trajectory tracking control problem. The control solution with \mathcal{L}_2 gain performance is presented in Section 3. Section 4 demonstrates the application of the proposed control scheme to a space robot. Conclusions are given in Section 5.

2. Preliminaries and Problem Formulation

The notation adopted in this paper is fairly standard. Let \mathfrak{R} (resp., \mathfrak{R}_+) denote the set of real (resp., positive real) numbers. The set of m by n real matrices is denoted as $\mathfrak{R}^{m \times n}$. For a given vector, $\|\cdot\|$ denotes the vector Euclidean norm; for a given matrix, $\|\cdot\|$ represents its induced Euclidean norm, and $\|\cdot\|_F$ denotes the matrix *Frobenius* norm. $\text{Tr}(\cdot)$ denotes the trace operator.

2.1. Definition. Our main results rely on the following stability definitions for a given nonlinear system:

$$\begin{aligned} \dot{\boldsymbol{\xi}}(t) &= \mathbf{f}(\boldsymbol{\xi}, t) + \mathbf{g}(\boldsymbol{\xi}, t) \mathbf{d}, \\ \mathbf{y} &= \mathbf{h}(\boldsymbol{\xi}, t), \end{aligned} \quad (1)$$

where $\mathbf{f}(\boldsymbol{\xi}, t): \mathfrak{R}^n \times \mathfrak{R}_+ \rightarrow \mathfrak{R}^n$ are locally Lipschitz and piecewise continuous in t and $\mathbf{d} \in \mathfrak{R}^s$ is an exogenous disturbance, while $\mathbf{y} \in \mathfrak{R}^m$ is the system output. We denote by $\boldsymbol{\xi}(\mathbf{x}_0, t_0, t)$ the solution to the nonlinear system (1) with the initial state \mathbf{x}_0 and initial time t_0 .

Definition 1 (see [18]). Let $\gamma > 0$ be a given constant; then system (1) is said to be achieved with \mathcal{L}_2 gain disturbance attenuation level of γ from external disturbance \mathbf{d} to output \mathbf{y} , if the following inequality holds:

$$V(t) - V(0) \leq \gamma^2 \int_0^t \|\mathbf{d}\|^2 dv - \int_0^t \|\mathbf{y}\|^2 dv, \quad (2)$$

where $V \in \mathfrak{R}$ is a Lyapunov candidate function to be chosen.

2.2. System Description of Space Robot. Consider n -link space robot with each joint driven by a dedicated, armature-controlled dc motor and operating in a free-floating mode.

Define $\mathbf{x} \in \mathfrak{R}^m$ ($m \leq n$) as the end-effector positive and attitude vector; then the space robot kinematics and dynamics can be described as

$$\dot{\mathbf{x}} = [\mathbf{J}_{G_0}(\mathbf{q}, \dot{\mathbf{q}}) + \Delta \mathbf{J}_G(\mathbf{q}, \dot{\mathbf{q}})] \dot{\mathbf{q}}_m, \quad (3)$$

$$\begin{aligned} &[\mathbf{M}_0(\mathbf{q}) + \Delta \mathbf{M}(\mathbf{q})] \ddot{\mathbf{q}}_m + \mathbf{C}_0(\mathbf{q}, \dot{\mathbf{q}}) \dot{\mathbf{q}}_m + \Delta \mathbf{C}(\mathbf{q}, \dot{\mathbf{q}}) \dot{\mathbf{q}}_m \\ &= \boldsymbol{\tau}_m + \boldsymbol{\tau}_d, \end{aligned} \quad (4)$$

where $\dot{\mathbf{x}} = [\mathbf{v}_e^T \ \boldsymbol{\omega}_e^T]^T \in \mathfrak{R}^m$ denotes the generalized velocity vector of the end-effector; here \mathbf{v}_e and $\boldsymbol{\omega}_e$ are the velocity and the angular velocity of the end-effector, respectively.

The vector $\mathbf{q} = [\mathbf{q}_0^T \ \mathbf{q}_m^T]^T \in \mathfrak{R}^n$ is the generalized coordinates. The term $\mathbf{J}_{G_0}(\mathbf{q}, \dot{\mathbf{q}}) \in \mathfrak{R}^n$ denotes the generalized but known/nominal Jacobian matrix, while $\Delta \mathbf{J}_G(\mathbf{q}, \dot{\mathbf{q}}) \in \mathfrak{R}^n$ is the uncertain Jacobian matrix. $\mathbf{M}_0(\mathbf{q}) \in \mathfrak{R}^{n \times n}$ is the nominal inertia matrix; $\Delta \mathbf{M}(\mathbf{q}) \in \mathfrak{R}^{n \times n}$ is the uncertain inertia. $\mathbf{C}_0(\mathbf{q}, \dot{\mathbf{q}}) \in \mathfrak{R}^n$ is the nominal vector of Coriolis and centrifugal forces, and $\Delta \mathbf{C}(\mathbf{q}, \dot{\mathbf{q}}) \in \mathfrak{R}^n$ denotes its uncertain part. $\boldsymbol{\tau}_m \in \mathfrak{R}^n$ is the vector of control torque, and $\boldsymbol{\tau}_d \in \mathfrak{R}^n$ is the vector of external disturbance.

To control the plant (3)-(4) successfully, the following assumption is assumed to be valid throughout this paper.

Assumption 2. The nominal Jacobian matrix $\mathbf{J}_{G_0}(\mathbf{q}, \dot{\mathbf{q}}) \in \mathfrak{R}^n$ and the matrix $\mathbf{M}_0^{-1}(\mathbf{q}) \in \mathfrak{R}^{n \times n}$ are bounded. There exist two positive scalars $\Delta_{\mathbf{J}_{G_0}} \in \mathfrak{R}_+$ and $\Delta_{\mathbf{M}_0^{-1}} \in \mathfrak{R}_+$ such that $\|\mathbf{J}_{G_0}(\mathbf{q}, \dot{\mathbf{q}})\| \leq \Delta_{\mathbf{J}_{G_0}}$ and $\|\mathbf{M}_0^{-1}(\mathbf{q})\| \leq \Delta_{\mathbf{M}_0^{-1}}$, respectively.

2.3. Chebyshev Neural Network. The Chebyshev neural network (CNN) [19] has been shown to be capable of universally approximating any well-defined functions over a compact set to any degree of accuracy. Therefore, CNN will be used to estimate the uncertain terms in the space robot dynamics. The CNN structure employed in this paper is with single layer and the Chebyshev polynomial basis function. This basis function is a set of Chebyshev differential equations and generated by the following two-term recursive formula:

$$\begin{aligned} T_{i+1}(x) &= 2xT_i(x) - T_{i-1}(x), \\ T_0(x) &= 1. \end{aligned} \quad (5)$$

In this paper, $T_1(x) = x$ is chosen. Define $\mathbf{X} = [x_1 \ x_2 \ \dots \ x_m]^T$; then the Chebyshev polynomial equation can be described as

$$\begin{aligned} \Theta(\mathbf{X}) &= [1, T_1(x_1), \dots, T_N(x_1), \dots, T_1(x_m), \dots, \\ &T_N(x_m)], \end{aligned} \quad (6)$$

where n is the order of Chebyshev polynomial chosen and $\Theta(\mathbf{X})$ is called the Chebyshev polynomial basis function.

As a result, for any continuous nonlinear function vector $\mathbf{f}_{Ni}(\mathbf{X}) \in \mathfrak{R}^n$, it can be approximated by CNN as

$$\mathbf{f}_{Ni}(\mathbf{X}) = (\mathbf{W}_i^*)^T \Theta_i(\mathbf{X}) + \boldsymbol{\varepsilon}_i, \quad (7)$$

where $\boldsymbol{\varepsilon}_i \in \mathfrak{R}_+^n$ is the bounded CNN approximation error, \mathbf{W}_i^* is an optimal weight matrix, and $\Theta_i(\mathbf{X})$ is the Chebyshev polynomial basis function.

Assumption 3. The optimal weight matrix \mathbf{W}_i^* is bounded. That is, there exists a positive constant $W_{Mi} \in \mathfrak{R}_+$ such that $\text{tr}((\mathbf{W}_i^*)^T \mathbf{W}_i^*) \leq W_{Mi}$.

2.4. Problem Statement. The objective of the proposed design methodology is to construct a control input function such that the end-effector trajectory state \mathbf{x} of the controlled system is capable of tracking a desired reference trajectory $\mathbf{x}_d \in \mathfrak{R}^n$ in spite of the existence of system uncertainties and external disturbances.

3. End-Effector Trajectory Tracking Control Design with Uncertain Kinematics and Dynamics

Because the system dynamics described in (3)-(4) cannot be linearized, CNN will be applied in this section to approximate the unknown system dynamics which can be not linearized in the system. Then, an adaptive backstepping control law will be presented to achieve trajectory tracking control for the space robot end-effector. Moreover, the tracking performance is evaluated by \mathcal{L}_2 gain from external disturbance/system uncertainties to the system outputs of the robot and desired trajectories.

3.1. Control Law Design with \mathcal{L}_2 Gain Performance. In the controller design, it is assumed that the trajectory of the space robot's end-effector is always within the Path Independent Workspace (PIW). All the points in the PIW are guaranteed not to have dynamic singularities. As a result, it can ensure that $\mathbf{J}_{G0}(\mathbf{q}, \dot{\mathbf{q}}) \in \mathfrak{R}^n$ will be always invertible.

Define the trajectory tracking error as

$$\mathbf{z}_1 = \mathbf{x} - \mathbf{x}_d. \quad (8)$$

Combining with the dynamics (3), it leads to the time derivative of \mathbf{z}_1 as

$$\dot{\mathbf{z}}_1 = \dot{\mathbf{x}} - \dot{\mathbf{x}}_d = \mathbf{J}_{G0} \dot{\mathbf{q}}_m + \mathbf{f}_1 - \dot{\mathbf{x}}_d, \quad (9)$$

where $\mathbf{f}_1(\mathbf{q}, \dot{\mathbf{q}}) = \Delta \mathbf{J}_G(\mathbf{q}, \dot{\mathbf{q}}) \dot{\mathbf{q}}_m$ denotes the uncertain kinematics.

To remove the effect of the above uncertain kinematics, CNN is used to approximate $\mathbf{f}_1(\mathbf{q}, \dot{\mathbf{q}})$; that is,

$$\mathbf{f}_1 = (\mathbf{W}_1^*)^T \Theta_1 + \boldsymbol{\varepsilon}_1, \quad (10)$$

where $\boldsymbol{\varepsilon}_1 \in \mathfrak{R}_+^n$ is the bounded CNN approximation error, \mathbf{W}_1^* is an optimal weight matrix, and Θ_1 is the Chebyshev polynomial basis function.

To accomplish controller design, a virtual control input is

$$\bar{\mathbf{q}}_m = \mathbf{J}_{G0}^{-1} \left(-k_1 \mathbf{z}_1 + \dot{\mathbf{x}}_d - \widehat{\mathbf{W}}_1^T \Theta_1 \right), \quad (11)$$

where $k_1 \in \mathfrak{R}_+$ is a constant and $\widehat{\mathbf{W}}_1^T$ is the estimate of the term $(\mathbf{W}_1^*)^T$ in (11).

Additionally, define an error vector for $\dot{\mathbf{q}}_m$ and $\bar{\mathbf{q}}_m$; that is,

$$\mathbf{z}_2 = \dot{\mathbf{q}}_m - \bar{\mathbf{q}}_m. \quad (12)$$

From the dynamics (4), one has

$$\dot{\mathbf{z}}_2 = \ddot{\mathbf{q}}_m - \ddot{\bar{\mathbf{q}}}_m = \mathbf{M}_0^{-1} (\boldsymbol{\tau}_m + \boldsymbol{\tau}_d - \mathbf{C}_0) + \mathbf{f}_2 - \ddot{\bar{\mathbf{q}}}_m, \quad (13)$$

where $\mathbf{f}_2(\mathbf{q}, \dot{\mathbf{q}}) = \ddot{\mathbf{q}}_m + \mathbf{M}_0^{-1} (\Delta \mathbf{C} - \mathbf{M} \ddot{\mathbf{q}}_m)$ denotes the uncertain dynamics. As the same technique applied to handle with uncertain kinematics, CNN will also be applied to approximate $\mathbf{f}_2(\mathbf{q}, \dot{\mathbf{q}})$. It thus follows that

$$\mathbf{f}_2 = (\mathbf{W}_2^*)^T \Theta_2 + \boldsymbol{\varepsilon}_2, \quad (14)$$

where $\boldsymbol{\varepsilon}_2 \in \mathfrak{R}_+^n$ is the bounded CNN approximation error, \mathbf{W}_2^* is an optimal weight matrix, and Θ_2 is the Chebyshev polynomial basis function.

Introduce two new variables $\mathbf{s} = \dot{\mathbf{x}} - \dot{\mathbf{x}}_d + k_1(\mathbf{x} - \mathbf{x}_d)$ and

$$\widehat{\mathbf{s}} = \mathbf{J}_{G0} \dot{\mathbf{q}}_m + \widehat{\mathbf{W}}_1^T \Theta_1 - \dot{\mathbf{x}}_d + k_1(\mathbf{x} - \mathbf{x}_d). \quad (15)$$

Then, it leads to $\mathbf{s} - \widehat{\mathbf{s}} = \widehat{\mathbf{W}}_1^T \Theta_1 + \boldsymbol{\varepsilon}_1$, where $\widehat{\mathbf{W}}_i$ is the estimate of the optimal weight matrix \mathbf{W}_i and $\widehat{\mathbf{W}}_i = \mathbf{W}_i^* - \widehat{\mathbf{W}}_i$ is the estimate error, $i = 1, 2$.

Theorem 4. Consider the space robot system described by (3)-(4) with external disturbance and system uncertainties; design $\boldsymbol{\tau}_m$ as

$$\begin{aligned} \boldsymbol{\tau}_m = & \mathbf{C}_0 + \mathbf{M}_0 \left(-k_2 \mathbf{z}_2 - \mathbf{J}_{G0}^T \mathbf{z}_1 - \varrho_1 \mathbf{J}_{G0}^T \widehat{\mathbf{s}} \right) \\ & + \mathbf{M}_0 \left(-\widehat{\mathbf{W}}_2^T \Theta_2 + \ddot{\bar{\mathbf{q}}}_m \right). \end{aligned} \quad (16)$$

Let $\widehat{\mathbf{W}}_i$ be updated by

$$\dot{\widehat{\mathbf{W}}}_1 = \frac{1}{\xi_1} \Theta_1 \mathbf{z}_1^T - \frac{\eta_1}{\xi_1} \|\mathbf{z}_1\|^2 \widehat{\mathbf{W}}_1, \quad (17)$$

$$\dot{\widehat{\mathbf{W}}}_2 = \frac{1}{\xi_2} \Theta_2 \mathbf{z}_2^T - \frac{\eta_2}{\xi_2} \|\mathbf{z}_2\|^2 \widehat{\mathbf{W}}_2, \quad (18)$$

where $k_2 \in \mathfrak{R}_+$ and $\varrho_1 \in \mathfrak{R}_+$ are two control gains and $\xi_1 \in \mathfrak{R}_+$, $\xi_2 \in \mathfrak{R}_+$, $\eta_1 \in \mathfrak{R}_+$, and $\eta_2 \in \mathfrak{R}_+$ are parameters for the adaptive laws. Suppose that the control parameters are chosen such that

$$k_1 \geq \lambda_1^2 + \frac{1}{4\gamma^2} + \frac{\eta_1 W_{M1}}{2}, \quad (19)$$

$$k_2 \geq \lambda_2^2 + \frac{1}{4\gamma^2} + \frac{\Delta_{B_0}^2}{4\gamma^2} - \varrho_1 \Delta_{J_{G0}}^2 + \frac{\eta_2 W_{M2}}{2}, \quad (20)$$

where λ_1 , λ_2 , and γ are positive constants. Then, the closed-loop attitude tracking system is guaranteed to be ultimately uniformly bounded. The \mathcal{L}_2 gain disturbance attenuation level is achieved. Moreover, when there is no external disturbance, the closed-loop system is asymptotically stable.

3.2. Stability Analysis. For the introduced variables, applying (12) and (15)-(17), the dynamics for \mathbf{z}_1 and \mathbf{z}_2 can be rewritten as

$$\begin{aligned} \dot{\mathbf{z}}_1 = & -k_1 \mathbf{z}_1 + \mathbf{J}_{G0} \mathbf{z}_2 + \widehat{\mathbf{W}}_1^T \Theta_1 + \boldsymbol{\varepsilon}_1, \\ \dot{\mathbf{z}}_2 = & -\mathbf{J}_{G0}^T \mathbf{z}_1 - k_2 \mathbf{z}_2 - \varrho_1 \mathbf{J}_{G0}^T \widehat{\mathbf{s}} + \mathbf{M}_0^{-1} \boldsymbol{\tau}_d + \widehat{\mathbf{W}}_2^T \Theta_2 \\ & - \boldsymbol{\varepsilon}_2. \end{aligned} \quad (21)$$

Proof of Theorem 4. Choose a Lyapunov candidate function as

$$V = \frac{1}{2} \sum_{i=1}^2 [\mathbf{z}_i^T \mathbf{z}_i + \xi_i \text{tr} \{ \widetilde{\mathbf{W}}_i^T \widetilde{\mathbf{W}}_i \}]. \quad (22)$$

Calculating the time derivative of V yields

$$\begin{aligned} \dot{V} = & \mathbf{z}_1^T [-k_1 \mathbf{z}_1 + \mathbf{J}_{G0} \mathbf{z}_2 + \widetilde{\mathbf{W}}_2^T \boldsymbol{\Theta}_2 + \boldsymbol{\varepsilon}_1] \\ & + \mathbf{z}_2^T [-\mathbf{J}_{G0}^T \mathbf{z}_1 - k_2 \mathbf{z}_2 - \varrho_1 \mathbf{J}_{G0}^T \widehat{\mathbf{s}} + \mathbf{M}_0^{-1} \boldsymbol{\tau}_d] \\ & + \mathbf{z}_2^T [\widetilde{\mathbf{W}}_2^T \boldsymbol{\Theta}_2 + \boldsymbol{\varepsilon}_2] + \xi_1 \text{tr} \{ \dot{\widetilde{\mathbf{W}}}_1^T \widetilde{\mathbf{W}}_1 \} \\ & + \xi_2 \text{tr} \{ \dot{\widetilde{\mathbf{W}}}_2^T \widetilde{\mathbf{W}}_2 \}. \end{aligned} \quad (23)$$

According to the properties of matrix trace, one has

$$\begin{aligned} \mathbf{z}_i^T \widetilde{\mathbf{W}}_i^T \boldsymbol{\Theta}_i &= \text{tr} (\mathbf{z}_i^T \widetilde{\mathbf{W}}_i^T \boldsymbol{\Theta}_i) = \text{tr} (\widetilde{\mathbf{W}}_i^T \boldsymbol{\Theta}_i \mathbf{z}_i^T) \\ \text{tr} (\widetilde{\mathbf{W}}_i^T \widetilde{\mathbf{W}}_i) &\leq \frac{1}{2} \text{tr} (\widetilde{\mathbf{W}}_i^T \widetilde{\mathbf{W}}_i) + \frac{1}{2} \text{tr} ((\mathbf{W}_i^*)^T \mathbf{W}_i^*) \\ &\quad - \text{tr} (\widetilde{\mathbf{W}}_i^T \widetilde{\mathbf{W}}_i) \\ &= \frac{1}{2} \text{tr} ((\mathbf{W}_i^*)^T \mathbf{W}_i^*) - \frac{1}{2} \text{tr} (\widetilde{\mathbf{W}}_i^T \widetilde{\mathbf{W}}_i). \end{aligned} \quad (24)$$

Applying (12) and (15), it can be obtained that

$$\mathbf{J}_{G0} \mathbf{z}_2 = \mathbf{J}_{G0} (\dot{\mathbf{q}}_m - \bar{\mathbf{q}}_m) = \widehat{\mathbf{s}}; \quad (25)$$

here $\dot{\widetilde{\mathbf{W}}}_i = -\dot{\widehat{\mathbf{W}}}_i$ is used.

Based on Assumption 2, it leaves (23) as follows:

$$\begin{aligned} \dot{V} \leq & -k_1 \|\mathbf{z}_1\|^2 - (k_2 + \varrho_1 \Delta_{J_{G0}}^2) \|\mathbf{z}_2\|^2 \\ & + \frac{\eta_1}{2} \|\mathbf{z}_1\|^2 \text{tr} \{ \mathbf{W}_1^{*T} \mathbf{W}_1^* \} - \frac{\eta_1}{2} \|\mathbf{z}_1\|^2 \text{tr} \{ \widetilde{\mathbf{W}}_1^T \widetilde{\mathbf{W}}_1 \} \\ & + \frac{\eta_2}{2} \|\mathbf{z}_2\|^2 \text{tr} \{ \mathbf{W}_2^{*T} \mathbf{W}_2^* \} - \frac{\eta_2}{2} \|\mathbf{z}_2\|^2 \text{tr} \{ \widetilde{\mathbf{W}}_2^T \widetilde{\mathbf{W}}_2 \} \\ & + \Delta_{B_0^{-1}} \mathbf{z}_2^T \boldsymbol{\tau}_d + \mathbf{z}_1^T \boldsymbol{\varepsilon}_1 + \mathbf{z}_2^T \boldsymbol{\varepsilon}_2. \end{aligned} \quad (26)$$

From Assumption 3, inequality (26) can be simplified as

$$\begin{aligned} \dot{V} \leq & - \left(k_1 - \frac{\eta_1 W_{M1}}{2} \right) \|\mathbf{z}_1\|^2 \\ & - \left(k_2 + \varrho_1 \Delta_{J_{G0}}^2 - \frac{\eta_2 W_{M2}}{2} \right) \|\mathbf{z}_2\|^2 \\ & - \frac{\eta_1}{2} \|\mathbf{z}_1\|^2 \|\widetilde{\mathbf{W}}_1\|_F^2 - \frac{\eta_2}{2} \|\mathbf{z}_2\|^2 \|\widetilde{\mathbf{W}}_2\|_F^2 \\ \leq & -\mu_1 \|\mathbf{z}_1\|^2 - \mu_2 \|\mathbf{z}_2\|^2 + \Delta_{B_0^{-1}} \mathbf{z}_2^T \boldsymbol{\tau}_d + \mathbf{z}_1^T \boldsymbol{\varepsilon}_1 + \mathbf{z}_2^T \boldsymbol{\varepsilon}_2, \end{aligned} \quad (27)$$

where $\mu_1 = k_1 - \eta_1 W_{M1}/2$ and $\mu_2 = k_2 + \varrho_1 \Delta_{J_{G0}}^2 - \eta_2 W_{M2}/2$.

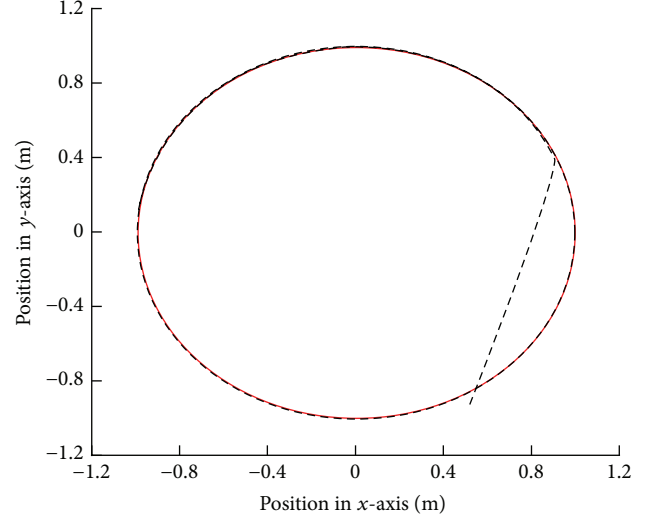


FIGURE 1: The desired trajectory (solid line) and the actual trajectory (dashed line) of end-effector with $k_1 = 10$ and $k_2 = 5$.

Define lumped disturbance as $\boldsymbol{\Gamma} = [\boldsymbol{\tau}_d^T \quad \boldsymbol{\varepsilon}_1^T \quad \boldsymbol{\varepsilon}_2^T]^T$ and system output as $\mathbf{y} = [\lambda_1 \mathbf{z}_1^T \quad \lambda_2 \mathbf{z}_2^T]^T$; then

$$\begin{aligned} H = \dot{V} + \mathbf{y}^T \mathbf{y} - \gamma^2 \boldsymbol{\Gamma}^T \boldsymbol{\Gamma} \\ \leq - \left(\mu_1 - \lambda_1^2 - \frac{1}{4\gamma^2} \right) \|\mathbf{z}_1\|^2 \\ - \left(\frac{\Delta_{B_0^{-1}}}{2\gamma} \|\mathbf{z}_2\| - \gamma \|\boldsymbol{\tau}_d\| \right)^2 \\ - \left(\mu_2 - \lambda_2^2 - \frac{1}{4\gamma^2} - \frac{\Delta_{B_0^{-1}}^2}{4\gamma^2} \right) \|\mathbf{z}_2\|^2 \\ - \left(\frac{1}{2\gamma} \|\mathbf{z}_1\| - \gamma \|\boldsymbol{\varepsilon}_1\| \right)^2 - \left(\frac{1}{2\gamma} \|\mathbf{z}_2\| - \gamma \|\boldsymbol{\varepsilon}_2\| \right)^2. \end{aligned} \quad (28)$$

With the choice of γ and the control gains in (19)-(20), it results in

$$\begin{aligned} \mu_1 &\geq \lambda_1^2 + \frac{1}{4\gamma^2}, \\ \mu_2 &\geq \lambda_2^2 + \frac{1}{4\gamma^2} + \frac{\Delta_{B_0^{-1}}^2}{4\gamma^2}. \end{aligned} \quad (29)$$

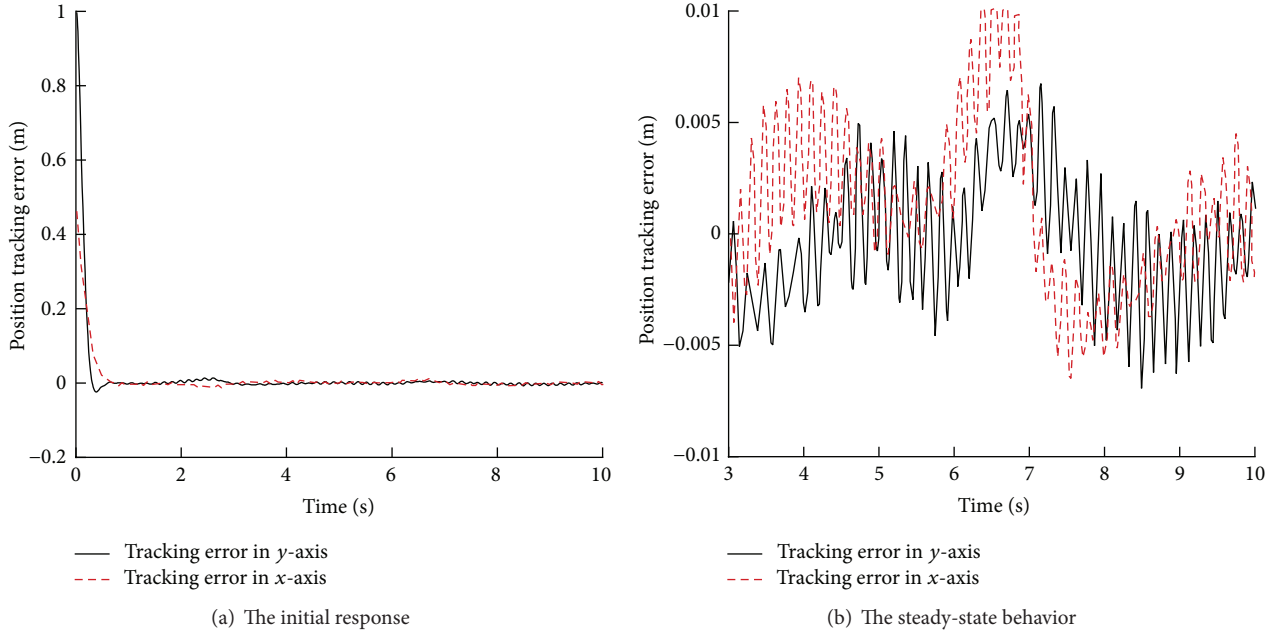
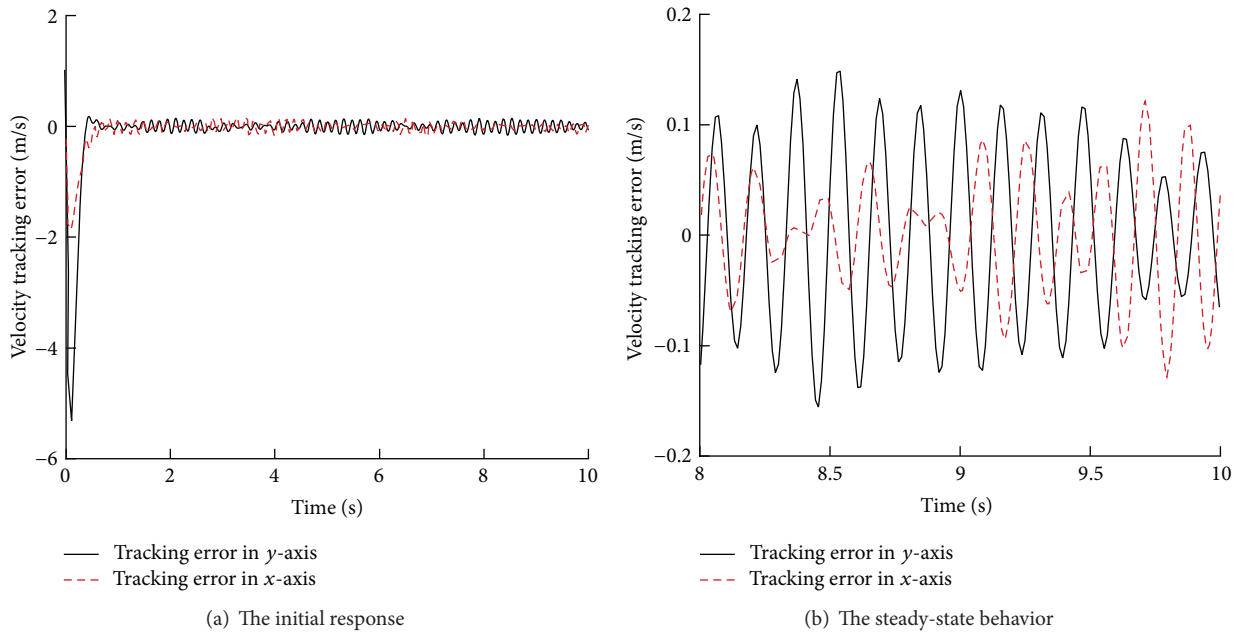
Then, it can be obtained from (28) that

$$H = \dot{V} + \mathbf{y}^T \mathbf{y} - \gamma^2 \boldsymbol{\Gamma}^T \boldsymbol{\Gamma} \leq 0. \quad (30)$$

By integrating inequality (30) from 0 to t , it can be shown that

$$V(t) - V(0) \leq \gamma^2 \int_0^t \|\boldsymbol{\Gamma}\|^2 dv - \int_0^t \|\mathbf{y}\|^2 dv. \quad (31)$$

Applying Definition 1, it can be concluded that the trajectory tracking is performed with \mathcal{L}_2 gain disturbance attenuation level, and the closed-loop system is ultimately uniformly bounded. Thereby the proof is completed here. \square


 FIGURE 2: The position tracking error of the end-effector with $k_1 = 10$ and $k_2 = 5$.

 FIGURE 3: The velocity tracking error of the end-effector with $k_1 = 10$ and $k_2 = 5$.

It should be stressed that the smaller the value of γ is, the better the disturbance attenuation capability will be obtained. To evaluate the \mathcal{L}_2 gain disturbance attenuation capability, the following index is defined:

$$\gamma^* = \sqrt{\frac{\int \|\mathbf{y}\|^2 dt}{\int \|\Gamma\|^2 dt}}. \quad (32)$$

From (32), it is known that smaller γ^* will lead to better disturbance attenuation performance.

Additionally, because the desired trajectory \mathbf{x}_d , the CNN approximation error $\boldsymbol{\varepsilon}_i$, $i = 1, 2$, and the external disturbance are bounded, there will exist a positive constant Γ_{\max} such that $\|\Gamma\| \leq \Gamma_{\max}$. Using the inequality $H \leq 0$, it yields

$$\begin{aligned} \dot{V} &\leq -\frac{1}{2} \|\mathbf{y}\|^2 + \gamma^2 \Gamma_{\max}^2 \\ &\leq -\frac{1}{2} \|\lambda_1 \mathbf{z}_1\|^2 - \frac{1}{2} \|\lambda_2 \mathbf{z}_2\|^2 + \gamma^2 \Gamma_{\max}^2. \end{aligned} \quad (33)$$

TABLE 1: Simulations parameters.

Physical name	Value
Space robot link	$m_0 = 40, m_1 = 3, m_2 = 4, b_2 = 0.5$ $a_2 = 0.5, a_1 = 0.5, b_1 = 0.5,$ $I_0 = 6.667, I_1 = 0.25, I_2 = 0.333$
Control gains	$k_1 = 10, k_2 = 5, \eta_1 = 0.5,$ $\eta_2 = 0.7, \xi_1 = 0.3, \xi_2 = 0.5, \rho_1 = 2.2$
The order of CNN	$n = 3$
The initial value of optimal weight matrix	$\mathbf{W}(0) = \mathbf{0}_{55 \times 6}$
External disturbance	$\boldsymbol{\tau}_d = a \begin{bmatrix} 2 \sin(n_c t) & \cos(2n_c t) & -4 \sin(n_c t) \end{bmatrix}^T$ $n_c = 0.02, a = 0.01$

Then, one has $\lim_{t \rightarrow \infty} \|\mathbf{z}_1\| \leq \gamma \Gamma_{\max} / \lambda_1$ and $\lim_{t \rightarrow \infty} \|\mathbf{z}_2\| \leq \gamma \Gamma_{\max} / \lambda_2$. It can thus obtain that \mathbf{z}_1 and \mathbf{z}_2 are bounded. More specifically, when $\boldsymbol{\Gamma} = \mathbf{0}$, it follows that $\|\mathbf{z}_1\| \rightarrow 0$ and $\|\mathbf{z}_2\| \rightarrow 0$. As a result, the end-effector trajectory will asymptotically follow the desired trajectory.

4. Numerical Example

To test the proposed controller, a two-link space robot operating in a free-floating mode is numerically simulated. The trajectory tracking control for its end-effector is performed. The main physical parameters, control gains, and external disturbances are listed in Table 1. The desired trajectory is a circle in XY plane with its radius equal to 1 m.

4.1. Response by Using Different Control Gains. With application of the proposed approach, Figure 1 shows that the controller successfully accomplishes the trajectory following mission of the space robot end-effector. As the position tracking error shown in Figure 2, good steady-state performance is guaranteed with minor overshoot. The velocity tracking error of end-effector is shown in Figure 3. Vibration with high-frequency is seen. That is induced by external disturbances. The corresponding estimates of the optimal weight matrix when using CNN to handle system uncertainties are illustrated in Figure 4. It is got to know that those estimates of CNN are all bounded.

As summarized in Theorem 4, the trajectory tracking performance is dependent on the control gains. Hence, simulation by using different control gains is further carried out. Figures 5, 6, and 7 show the trajectory tracking error by using $k_1 = 1, k_2 = 5$; $k_1 = 3, k_2 = 5$; and $k_1 = 15, k_2 = 5$, respectively. From Figures 5~7, it is seen that larger value of k_1 will lead to fast convergence rate of the tracking error. Figure 8 shows the control performance by using $k_1 = 10$ and $k_2 = 50$. It is obtained from those results that larger value of k_2 cannot increase the response rate of the system when k_1 has a fixed value. Therefore, to ensure that the actual trajectory of the end-effector can follow the desired trajectory in a faster rate, the designer should choose k_1, k_2 to satisfy (17) and (20),

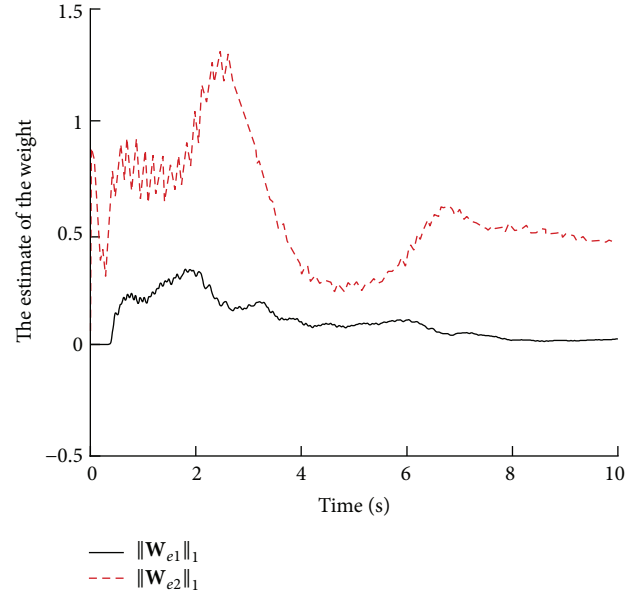


FIGURE 4: The estimate of the optimal weight matrix ($\widehat{\mathbf{W}}_1 = \mathbf{W}_{e1}$ and $\widehat{\mathbf{W}}_2 = \mathbf{W}_{e2}$) with $k_1 = 10$ and $k_2 = 5$.

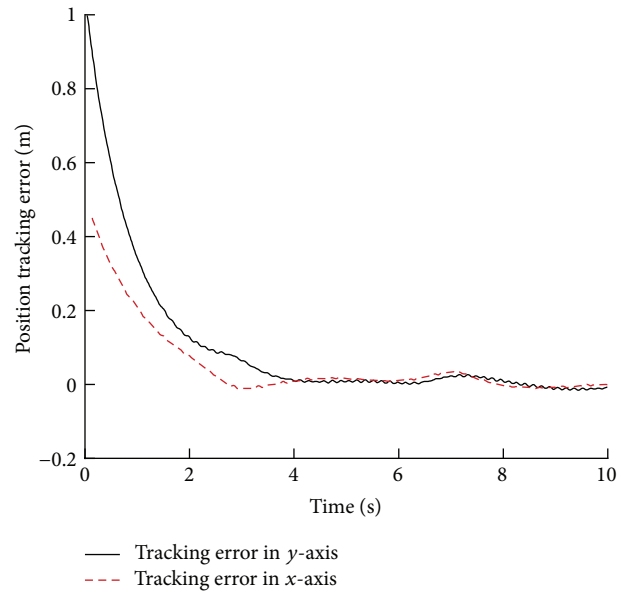


FIGURE 5: The position tracking error of the end-effector with $k_1 = 1$ and $k_2 = 5$.

respectively. At this time, choosing larger k_1 will result in that the desired trajectory will be followed in a shorter time. However, the maximum control effort of actuator should be taken into account when choosing k_1 .

4.2. Performance in the Absence of External Disturbances. In this case, an ideal condition is considered. That is, there are no external disturbances acting on the space robot. By using

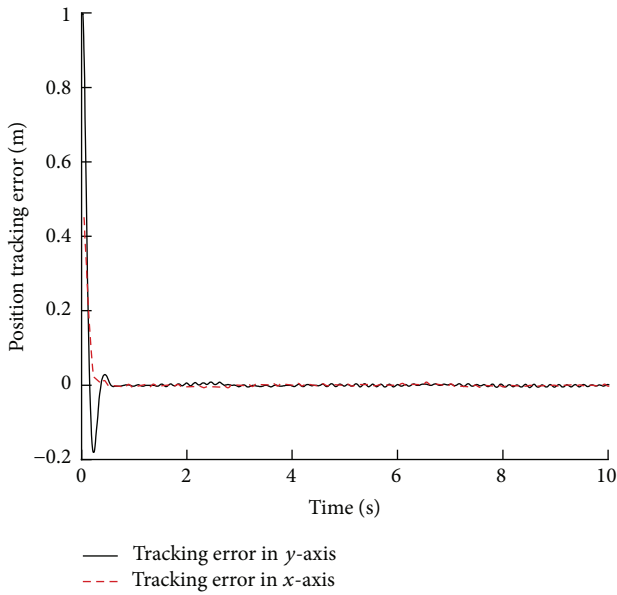


FIGURE 6: The position tracking error of the end-effector with $k_1 = 15$ and $k_2 = 5$.

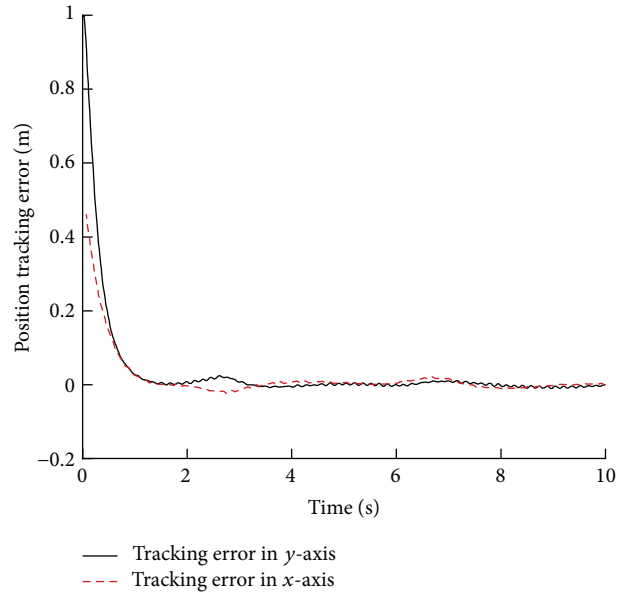


FIGURE 8: The position tracking error of the end-effector with $k_1 = 3$ and $k_2 = 5$.

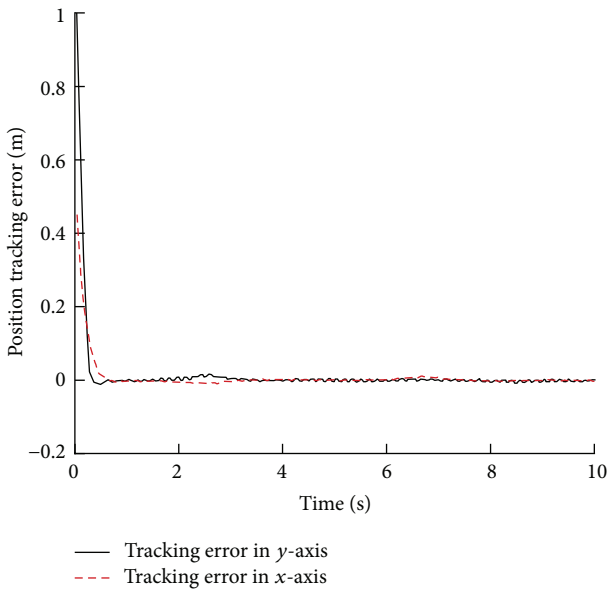


FIGURE 7: The position tracking error of the end-effector with $k_1 = 10$ and $k_2 = 50$.

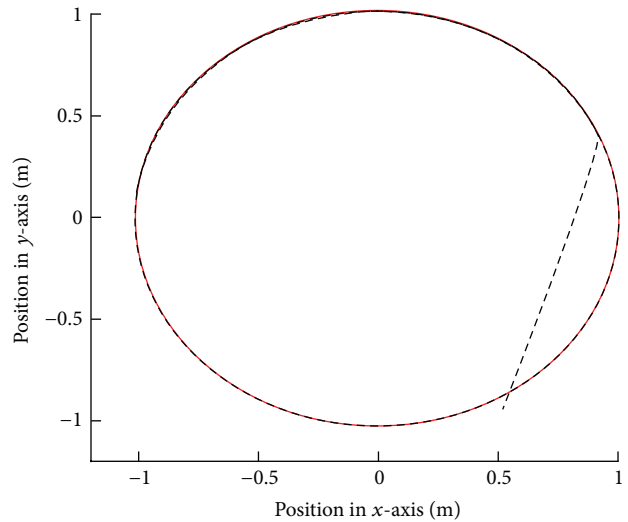


FIGURE 9: The desired trajectory (solid line) and the actual trajectory (dashed line) of end-effector in the absence of external disturbances.

the proposed control law, the control performance is shown in Figures 9~12. Those results demonstrate the conclusion in Theorem 4 that an asymptotic tracking can be guaranteed in the absence of external disturbances. Comparing Figures 2~4 with Figures 10~12, respectively, fewer overshoots are obtained in the absence of disturbances compared to those in the presence of external disturbances.

5. Conclusions

The problem of end-effector trajectory tracking control was investigated for a space robot working in free-floating mode by incorporating the criterion of a tracking performance given by \mathcal{L}_2 gain constraint in controller synthesis. External disturbance and system uncertainties were addressed. The proposed adaptive control approach was able to achieve high tracking performance even in the presence of uncertain kinematics and dynamics. The closed-loop tracking system

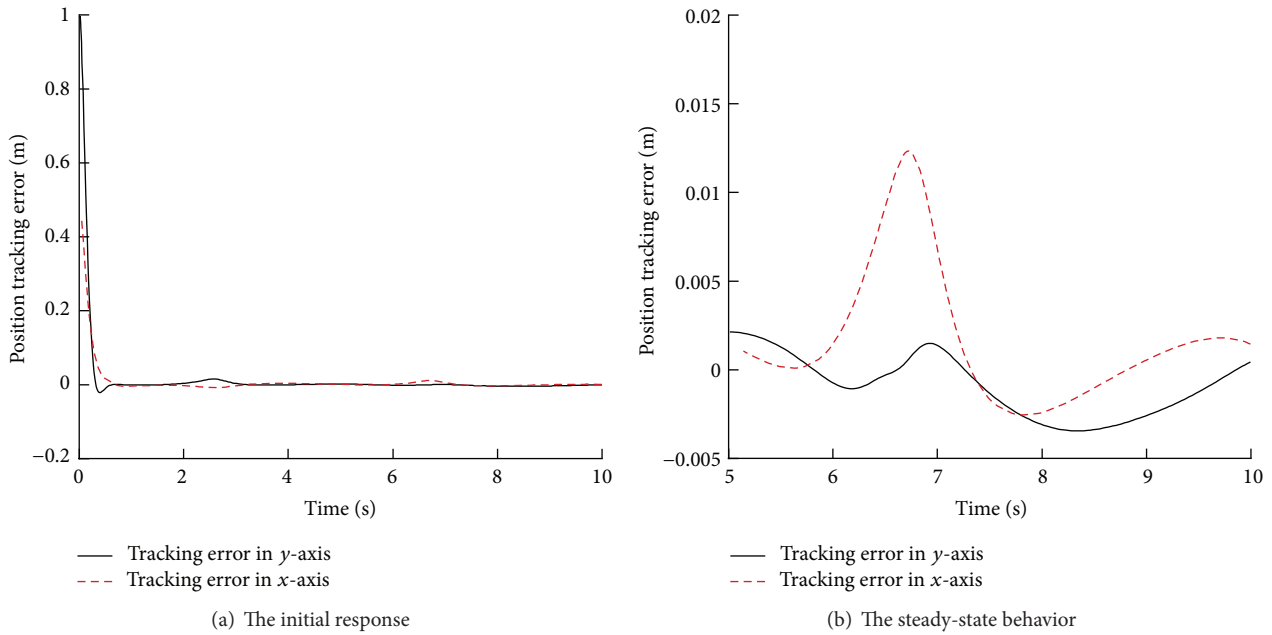


FIGURE 10: The position tracking error of end-effector in the absence of external disturbances.

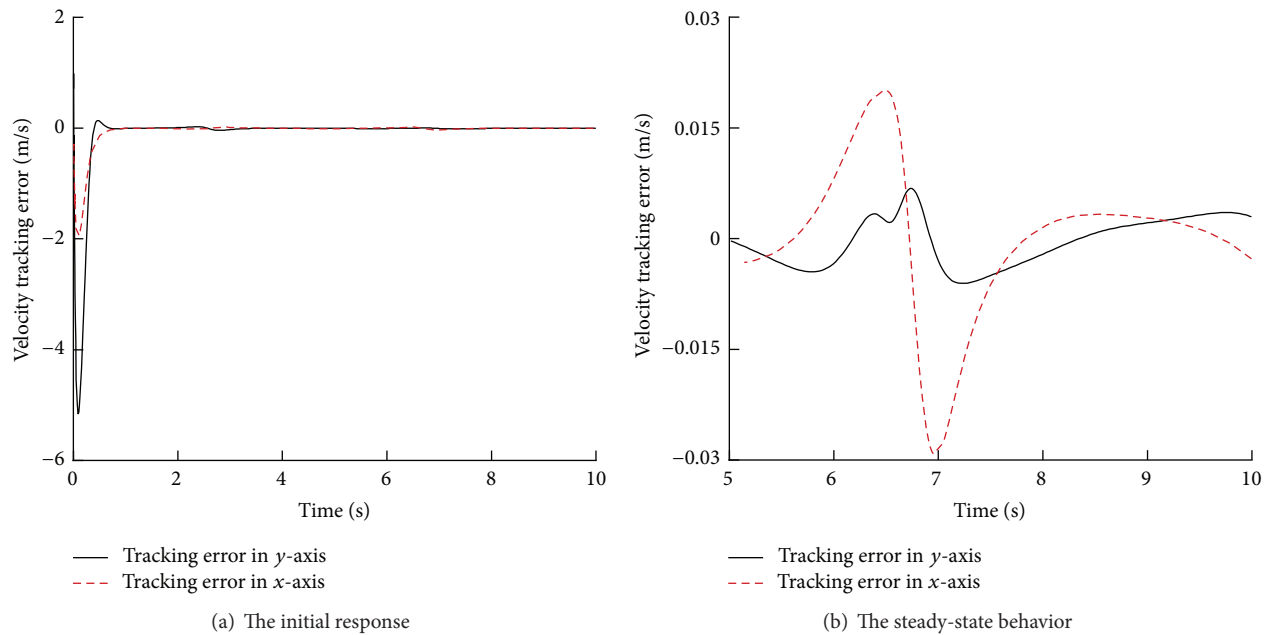


FIGURE 11: The velocity tracking error of end-effector in the absence of external disturbances.

was ensured to be global uniform ultimate bounded stable with the \mathcal{L}_2 gain less than any given small level. Moreover, when the space robot was not under the effect of any disturbance, the desired trajectory can be asymptotically followed. It should be pointed out that actuators are assumed to run normally when implementing the proposed approach. However, this assumption may not be satisfied in practice. As one

of future works, trajectory tracking control with fault tolerant capability should be carried out for space robot's end-effector.

Conflict of Interests

The authors declare that there is no conflict of interests regarding the publication of this paper.

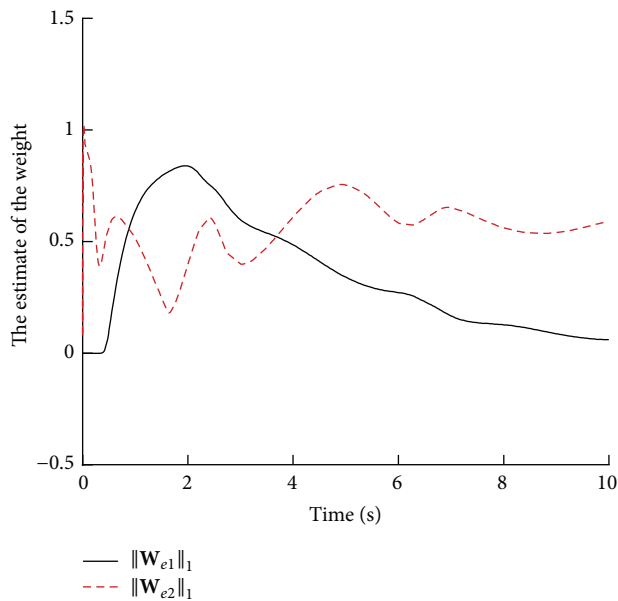


FIGURE 12: The estimate of the optimal weight matrix ($\widehat{W}_1 = W_{e1}$ and $\widehat{W}_2 = W_{e2}$) in the absence of external disturbances.

Acknowledgments

This work was supported partially by the National Natural Science Foundation of China (Project nos. 61503035 and 61573071) and the Foundation of the National Key Laboratory of Science and Technology on Space Intelligent Control (Project no. 9140C590202140C59015). The authors highly appreciate the preceding financial supports. The authors would also like to thank the reviewers and the editor for their valuable comments and constructive suggestions that helped to improve the paper significantly.

References

- [1] A. Flores-Abad, O. Ma, K. Pham, and S. Ulrich, "A review of space robotics technologies for on-orbit servicing," *Progress in Aerospace Sciences*, vol. 68, pp. 1–26, 2014.
- [2] W. Xu, B. Liang, and Y. Xu, "Survey of modeling, planning, and ground verification of space robotic systems," *Acta Astronautica*, vol. 68, no. 11–12, pp. 1629–1649, 2011.
- [3] D. L. Akin, J. C. Lanef, B. J. Roberts, and S. R. Weisman, "Robotic capabilities for complex space operations," in *Proceedings of the AIAA Space Conference and Exposition*, pp. 1–11, Albuquerque, NM, USA, August 2001.
- [4] L. M. Capisani, A. Ferrara, A. F. de Loza, and L. M. Fridman, "Manipulator fault diagnosis via higher order sliding-mode observers," *IEEE Transactions on Industrial Electronics*, vol. 59, no. 10, pp. 3979–3986, 2012.
- [5] S. Kim, A. Shukla, and A. Billard, "Catching objects in flight," *IEEE Transactions on Robotics*, vol. 30, no. 5, pp. 1049–1065, 2014.
- [6] S. Kim and A. Billard, "Estimating the non-linear dynamics of free-flying objects," *Robotics and Autonomous Systems*, vol. 60, no. 9, pp. 1108–1122, 2012.
- [7] C. C. Cheah, S. Kawamura, and S. Arimoto, "Feedback control for robotic manipulator with uncertain kinematics and dynamics," in *Proceedings of the IEEE International Conference on Robotics and Automation*, vol. 4, pp. 3607–3612, Leuven, Belgium, May 1998.
- [8] C. C. Cheah, M. Hirano, S. Kawamura, and S. Arimoto, "Approximate Jacobian control for robots with uncertain kinematics and dynamics," *IEEE Transactions on Robotics and Automation*, vol. 19, no. 4, pp. 692–702, 2003.
- [9] W. E. Dixon, "Adaptive regulation of amplitude limited robot manipulators with uncertain kinematics and dynamics," in *Proceedings of the American Control Conference (AAC '04)*, pp. 3839–3844, Boston, Mass, USA, July 2004.
- [10] C. C. Cheah, C. Liu, and J. J. E. Slotine, "Approximate Jacobian adaptive control for robot manipulators," in *Proceedings of the IEEE International Conference on Robotics and Automation (ICRA '04)*, vol. 3, pp. 3075–3080, IEEE, New Orleans, La, USA, April–May 2004.
- [11] X. Liang, X. Huang, M. Wang, and X. Zeng, "Adaptive task-space tracking control of robots without task-space- and joint-space-velocity measurements," *IEEE Transactions on Robotics*, vol. 26, no. 4, pp. 733–742, 2010.
- [12] C. C. Cheah, C. Liu, and J. J. E. Slotine, "Adaptive Jacobian tracking control of robots with uncertainties in kinematic, dynamic and actuator models," *IEEE Transactions on Automatic Control*, vol. 51, no. 6, pp. 1024–1029, 2006.
- [13] L. Cheng, Z.-G. Hou, and M. Tan, "Adaptive neural network tracking control for manipulators with uncertain kinematics, dynamics and actuator model," *Automatica*, vol. 45, no. 10, pp. 2312–2318, 2009.
- [14] A. J. van der Schaft, " L_2 -gain analysis of nonlinear systems and nonlinear state-feedback H_∞ control," *IEEE Transactions on Automatic Control*, vol. 37, no. 6, pp. 770–784, 1992.
- [15] M. Fujita, H. Kawai, and M. W. Spong, "Passivity-based dynamic visual feedback control for three-dimensional target tracking: stability and L_2 -gain performance analysis," *IEEE Transactions on Control Systems Technology*, vol. 15, no. 1, pp. 40–52, 2007.
- [16] C. Ishii, T. Shen, and Z. Qu, "Lyapunov recursive design of robust adaptive tracking control with L_2 -gain performance for electrically-driven robot manipulators," *International Journal of Control*, vol. 74, no. 8, pp. 811–828, 2001.
- [17] H. K. Khalil and J. Grizzle, *Nonlinear Systems*, Macmillan, New York, NY, USA, 1992.
- [18] A. van der Schaft, *L_2 -Gain and Passivity Techniques in Nonlinear Control*, Communications and Control Engineering, Springer, London, UK, 2nd edition, 2000.
- [19] A.-M. Zou and K. D. Kumar, "Adaptive attitude control of spacecraft without velocity measurements using Chebyshev neural network," *Acta Astronautica*, vol. 66, no. 5–6, pp. 769–779, 2010.



Hindawi

Submit your manuscripts at
<http://www.hindawi.com>

